

## Electrospinning nanofibers for wound healing using antioxidant from Rang Jued (*Thunbergia laurifolia* Lindl.) extract via subcritical fluid extraction

Nichapa Areepong and Veronica Winoto\*

Department of Chemical Engineering, Thammasat School of Engineering, Faculty of Engineering, Thammasat University, Pathumthani 12120, Thailand

Received 30 May 2025  
Revised 29 September 2025  
Accepted 1 October 2025

### Abstract

Rang Jued (*Thunbergia laurifolia* Lindl.) is a local Thai plant known for its bioactive compounds. In this study, subcritical ethanol extraction was used to extract antioxidant from Rang Jued (RJ) leaves. A total of 15 experiments were designed using Box-Behnken design. Response surface methodology was employed to determine the optimal condition, which yielded the highest DPPH scavenging activity of 94.91% and a total phenolic content of 30.35 mg GAE/g under the conditions of 1.64 g of Rang Jued powder, an extraction temperature of 190 °C, and an extraction time of 15.14 minutes. Furthermore, the electrospinning technique was used to fabricate antioxidant wound dressing nanofibers. The process was conducted by varying the ratio between PVA and RJ extract, as well as the voltage supply. Scanning electron microscopy (SEM) was used to investigate the morphology of the nanofibers. The average diameter ranged from 248 to 362 nm. The highest antioxidant activity of the nanofibers was observed at 72.25%, using a PVA:RJ extract ratio of 7:3 and a voltage of 40 kV.

**Keywords:** Antioxidants, Electrospinning process, Phenolic compounds, Subcritical fluid technique, *Thunbergia laurifolia* Lindl

### 1. Introduction

Herbal plants have been extensively used in Thailand due to their medicinal and biological properties. In many rural regions, people commonly rely on herbal plants to treat various ailments. This widespread use drew researchers' attention to Thai medicinal plants, particularly because of their phytochemical compositions. Several plants were studied for their biological activities and antioxidant properties, including *Aegle marmelos* (Bael fruit), *Stevia rebaudiana* (sweet leaves), *Pandanus amaryllifolius* (pandan leaves), *Thunbergia laurifolia* (Rang Jued), and *Morus alba* (mulberry) [1, 2]. Notably, Rang Jued was found to be rich in phytochemicals and was considered to have significant potential [3]. As a result, it became a focus in various research studies.

Rang Jued (*Thunbergia laurifolia* Lindl.) is a native Thai plant from the Acanthaceae family. It is commonly known as laurel clock vine due to its trumpet-shaped flowers, which appear in three colors: white, yellow, and purple. The purple-flowered variety of Rang Jued is particularly noted for its medicinal properties, with the stems, roots, and leaves used for various pharmacological purposes [4, 5]. In Thailand, Rang Jued is widely processed into products such as herbal teas, powders, and capsules, and is often recommended by Thai medical practitioners to help treat addiction to alcohol, drugs, and food poisoning [3].

Research has shown that extracts from Rang Jued, especially its leaves, possess several biological activities: (1) anti-inflammatory properties, where aqueous extracts of Rang Jued leaves were found to be more effective than mangosteen rind extract; (2) anti-diabetic effects, with studies showing that aqueous leaf extract can lower blood glucose levels in diabetic rats; (3) detoxification capabilities, where the leaf extract have been reported to reduce cadmium toxicity and prevent lead-induced neurotoxicity; and (4) antioxidant properties, with Rang Jued extract demonstrating high levels of total phenolic contents (TPC) and DPPH activities [4].

Moreover, Rang Jued extract contains various phenolic compounds, including rosmarinic acid, caffeic acid, gallic acid, quercetin, catechin, and rutin. Studies have identified rosmarinic acid as the primary antioxidant in Rang Jued [3] and additional research has confirmed that both rosmarinic and caffeic acids are the dominant antioxidants [6]. A study on the quantitative analysis of *Thunbergia laurifolia* reported the presence of caffeic acid, vicenin-2, and rosmarinic acid [7]. Furthermore, a study on the antioxidant activities of *Thunbergia laurifolia* Lindl. leaf extracts for skin aging and damage prevention reported that rosmarinic acid and flavonoids were the most abundant compounds, supporting its role as a natural anti-ageing ingredient [8].

Additionally, when polyphenols and antioxidant activities were studied in infused tea made from Rang Jued, significant levels of total phenolic contents (TPC) and total flavonoid content (TFC) were observed, along with a notable DPPH inhibitory effect [3]. Recently, several extraction methods have been developed, including Soxhlet, maceration, microwave-assisted, ultrasound-assisted, supercritical, and subcritical techniques using various solvents [9]. Previous studies showed that maceration of Rang Jued resulted in high total phenolic contents (TPC) and DPPH inhibition of over 85%, with rosmarinic acid concentrations of  $1896.7 \pm 89.3$  mg/100 g in leaves and caffeic acid at  $13.2 \pm 0.7$  mg/100 g. Another study reported rosmarinic acid levels of  $38.82 \pm 2.54$  mg/g dry weight with

\*Corresponding author.

Email address: wveronic@engr.tu.ac.th  
<https://doi.org/10.64960/easr.2026.262381>

maceration extraction [6]. Additionally, Rang Jued has been successfully extracted through an infused tea process, yielding high TPC levels ranging from  $709.7 \pm 1.36$  to  $744.8 \pm 5.79$  mg GAE/l [3].

Moreover, one increasingly popular method in research is the subcritical fluid technique. This innovative method operates with fluids under their critical point but above their boiling point, such as ethanol at  $78.3^{\circ}\text{C}$ , water at  $100^{\circ}\text{C}$ , methanol at  $64.7^{\circ}\text{C}$ , and acetone at  $56^{\circ}\text{C}$ . The technique offers advantages such as shorter extraction times, environmental friendliness, and high-quality extracts [10]. For example, subcritical ethanol extraction has been shown to recover oil from coconut meal with higher TPC and DPPH activity compared to Soxhlet extraction with hexane, indicating its effectiveness in preserving antioxidant properties [11]. Studies on defatted rice bran demonstrated that subcritical aqueous ethanol was more efficient than subcritical water under the same extraction conditions [12]. However, no research has yet explored subcritical extraction for Rang Jued, indicating that this technique holds significant potential for further exploration.

The electrospinning technique is widely used to produce nanofibers with diameters ranging from the micrometer to the nanometer scale [13]. Nanofibers are fabricated to exhibit properties such as a large surface area, high porosity, small diameter, and high air permeability [14]. Due to these characteristics, nanofibers have been applied in various fields, including tissue engineering, wound dressing, drug delivery, food packaging, and filtration [15].

Previous studies have demonstrated the use of electrospun nanofiber mats in food packaging to extend shelf life. For example, nanofibers loaded with black tea extract and polyvinyl alcohol (PVA) were designed to release polyphenols for this purpose [16]. In addition, nanofibers containing PVA and *Lepidium sativum* extract were applied as a wound dressing by incorporating antioxidant properties [14]. Studies on PVA loading with *Achillea millefolium* and *Viola* extracts as wound dressings exhibited excellent mechanical properties, antibacterial efficiency, and significant wound healing potential [17]. Nanofibers made from *Spirulina* and PCL (Polycaprolactone) were fabricated for wound dressing applications. *Spirulina*, known for its antioxidant activity, was used to prevent reactive oxygen species (ROS) stress through antioxidant mechanisms. Moreover, *Spirulina* extract accelerated wound regeneration [18]. Ginger- and thyme-loaded nanofiber were shown to protect against oxidative stress and promote wound healing, with DPPH inhibition ranging from 19.8 to 96.5% [19]. Nanofibers loaded with flaxseed extract demonstrated antioxidant activity ranging from 35% to 75%, which helped avert oxidative stress and supported wound healing [20].

Furthermore, electrospinning is a versatile technique that can be applied to various polymers, including polyvinyl alcohol (PVA), polylactic acid (PLA), polyethylene oxide (PEO), and others. Polyvinyl alcohol (PVA) has been widely used in the biomedical field due to its non-toxicity, biocompatible, biodegradable, and water solubility [13, 20]. Additionally, PVA can form a strong adhesive layer on the surface of polymers, which is beneficial for wound dressing applications [21]. Wound healing is typically categorized into four stages: (1) bleeding and hemostasis, (2) inflammation, (3) proliferation, and (4) tissue remodeling [22]. When the skin is damaged, reactive oxygen species (ROS) are generated during the inflammatory phase, damaging biological structures and hindering the healing process. Antioxidants can eliminate free radicals; therefore, loading antioxidant extract into nanofibers may accelerate wound healing [23].

*Thunbergia laurifolia* has been reported to exhibit both antioxidant activity and anti-inflammatory activities, which can help mitigate the inflammatory phase [24, 25]. For effective nanofiber dressings, good water solubility is essential. Therefore, crosslinking techniques play a crucial role in enhancing the stability and performance of nanofibers. Glutaraldehyde (GA) is an effective aldehyde-based crosslinking agent, widely used due to its low cytotoxic [26, 27]. However, GA crosslinking requires a closed vessel and extended reaction times [28]. To enhance the effectiveness of wound treatment, wound dressings should incorporate bioactive compounds. In this context, nanofibers can be loaded with Rang Jued extract using an optimized technique to maximize their therapeutic potential.

In this study, Rang Jued was extracted using subcritical extraction with ethanol as the solvent. The effects of temperature, extraction time, and the amount of Rang Jued powder were varied to determine optimal conditions using response surface methodology (RSM). Additionally, nanofibers were fabricated using the electrospinning technique, with varying PVA:Rang Jued extract ratios and applied voltages. The resulting nanofibers were analyzed for swelling behavior, crosslinking efficiency, fiber diameter, DPPH scavenging activity, and total phenolic content (TPC).

## 2. Materials and methods

### 2.1 Chemicals and materials

Ethanol (99.99%,  $\text{C}_2\text{H}_5\text{OH}$ , EtOH), methanol (99.8%,  $\text{CH}_3\text{OH}$ , MeOH), polyvinyl alcohol (PVA), Folin–Ciocalteu reagent, gallic acid monohydrate ( $\text{C}_7\text{H}_6\text{O}_5 \cdot \text{H}_2\text{O}$ ), sodium carbonate ( $\text{Na}_2\text{CO}_3$ ), and 2,2-diphenyl-1-picrylhydrazyl (DPPH) were purchased from QREC Thailand Asia, Thailand. *Thunbergia laurifolia* Lindl. (Rang Jued) leaves were sourced from Sisaket Province, Thailand.

### 2.2 *Thunbergia laurifolia* Lindl. (Rang Jued leaves) preparation

Rang Jued fresh leaves were washed with distilled water until cleaned. The cleaned leaves were then evenly spread on trays and dried in a hot-air oven at  $80^{\circ}\text{C}$  for 1.5 hours, with the fan operating at 100% speed. This controlled drying method was chosen to stabilize the material, thereby extending shelf-life, and eliminating moisture, resulting in a stable powder. After drying, the leaves were ground into a fine powder using a stainless steel mortar and pestle, followed by sieving. The resulting Rang Jued powder was stored in a desiccator.

### 2.3 Subcritical extraction using Box–Behnken design

A Box–Behnken design (BBD) was used to optimize DPPH scavenging activity and TPC based on three independent variables: the amount of Rang Jued powder, extraction temperature, and extraction time. The amount of Rang Jued powder ranged from 1.5 to 1.9 g, extraction temperature ranged from 160 to  $240^{\circ}\text{C}$ , and extraction time ranged from 5 to 25 min.

A total of 15 experimental runs were conducted using three levels of each variable. These levels were coded as  $-1$  for the low level,  $0$  for the middle level, and  $+1$  for the higher level, as shown in Table 1. The response variables from each experiment were fitted to a second-order polynomial equation derived from response surface methodology (RSM), as follows:

$$Y = \beta_0 + \beta_1 X_1 + \beta_2 X_2 + \beta_3 X_3 + \beta_{11} X_1^2 + \beta_{22} X_2^2 + \beta_{33} X_3^2 + \beta_{12} X_1 X_2 + \beta_{13} X_1 X_3 + \beta_{23} X_2 X_3 \quad (1)$$

where  $Y$  represents the response value of DPPH and TPC;  $X_1$ ,  $X_2$ , and  $X_3$  are the independent variables (amount of Rang Jued powder, temperature, and time);  $\beta_0$  is the model intercept coefficient,  $\beta_1$ ,  $\beta_2$ , and  $\beta_3$  are the linear coefficients;  $\beta_{11}$ ,  $\beta_{22}$ , and  $\beta_{33}$  are the quadratic coefficients;  $\beta_{12}$ ,  $\beta_{13}$ , and  $\beta_{23}$  are interaction coefficients of the second-order terms.

**Table 1** Range of variables and code levels for subcritical extraction using Box–Behnken design.

Variables	Coded levels		
	-1	0	+1
Rang Jued powder ( $X_1$ , g/50 ml EtOH)	1.5	1.7	1.9
Temperature ( $X_2$ , °C)	160	200	240
Time ( $X_3$ , min)	5	15	25

#### 2.4 Electrospinning process

A PVA solution was prepared at a concentration of 10% (w/v). The PVA was dissolved in distilled water using a magnetic stirrer at 80 °C for 3 h. Then, the PVA solution was mixed with Rang Jued (RJ) extract at three different volume ratios (%v/v): 7:3, 8:2, and 9:1. The mixtures were stirred for 15 minutes.

The electrospinning process was then used to fabricate PVA/RJ nanofibers using Nanospider™ technology. This technology employed an electrospinning electrode in the shape of a thin wire to apply a mixed polymer solution along its length. The electrospinning parameters included applied voltages of 30, 35, and 45 kV, an electrode-to-substrate distance of 240 mm, and a spinning electrode width of 300 mm.

A 10 ml portion of the prepared PVA/RJ solution was loaded into the carriage, which was positioned appropriately with the wire electrode. Finally, the resulting nanofiber mats were stored in a desiccator for further characterization.

#### 2.5 Crosslinking of nanofiber mats

Nanofiber mats (PVA/RJ) were crosslinked using 15 ml of glutaraldehyde (GA) solution. The mats and GA solution were placed in a vacuum box and heated at 40 °C for 24 h. After crosslinking, residual GA was removed by placing the mats in a fume hood for 30 min.

#### 2.6 Swelling characterization

The nanofiber mat was cut into 2 cm × 2 cm pieces, and the dry sample was weighed ( $W_{dm}$ ). The swelling behavior of the nanofiber mats was evaluated in phosphate-buffered saline (PBS) at pH 7.4. Each 2 cm<sup>2</sup> mat was placed in 3 ml of PBS for 24 h at room temperature. After incubation, the surface of each mat was gently wiped to remove excess PBS, and the sample was weighed ( $W_m$ ). All experiments were performed in triplicate. The degree of swelling was calculated using Equation 2 [29, 30]:

$$\text{Degree of swelling (\%)} = \left[ \frac{(W_m - W_{dm})}{W_{dm}} \right] \times 100 \quad (2)$$

where  $W_m$  is the weight of the sample after submersion, and  $W_{dm}$  is the weight of the dry sample.

#### 2.7 1,1-Diphenyl-2-picrylhydrazyl (DPPH) assay

The DPPH activity of the extract solution was determined by DPPH assay [31]. Briefly, a methanolic DPPH solution was prepared by dissolving 10 mg of DPPH in 100 ml of methanol and storing it in the dark. Then, 100 µl of the extract solution was mixed with 3 ml of DPPH solution. The mixture was incubated in the dark at room temperature for 30 min. Subsequently, the control solution was prepared by mixing 3 ml of DPPH solution with 100 µl of methanol. The absorbance was measured using UV–VIS spectrophotometer (V-1500/UV1500, Metash, Shanghai, China) at 517 nm. The percentage of DPPH inhibition was calculated using Equation 3:

$$\text{DPPH(\%)} = \left( \frac{\text{Abs}_{\text{control}} - \text{Abs}_{\text{sample}}}{\text{Abs}_{\text{control}}} \right) \times 100 \quad (3)$$

where  $\text{Abs}_{\text{control}}$  is the absorbance of the control solution, and  $\text{Abs}_{\text{sample}}$  is the absorbance of the sample solution.

The antioxidant activity of the nanofiber mats was also evaluated using the same procedure. After 24 h of the swelling test, 100 µl of the PBS solution was mixed with 3 ml of the DPPH solution, and the absorbance of the resulting mixture was measured to analyze the extract.

#### 2.8 Total phenolic contents (TPC) analysis

The total phenolic contents (TPC) were determined using the Folin–Ciocalteu method [32]. A 1 ml aliquot of the extract solution was added to a test tube, followed by 1 ml of Folin–Ciocalteu reagent. The mixture was left at room temperature for 5 min. Then, 10 ml of Na<sub>2</sub>CO<sub>3</sub> (7% w/v) was added. After mixing, the solution was incubated for 1 h. Absorbance was measured at 750 nm using a UV–VIS spectrophotometer (V-1500/UV1500, Metash, Shanghai, China).

Gallic acid was used as the standard for the calibration curve, with concentrations of 0, 5, 10, 20, 40, 60, 80, 100, 200, and 300 µg/ml. TPC was expressed as mg gallic acid equivalent per gram of sample (mg GAE/g).

Additionally, the nanofiber mats were analyzed for TPC. After swelling tests, 1 ml of the PBS solution was added to a test tube containing the mats, followed by Folin–Ciocalteu reagent and Na<sub>2</sub>CO<sub>3</sub> using the same procedure as for the extract samples. TPC in the nanofiber mats was calculated by comparison with the gallic acid calibration curve and expressed as mg GAE/g.

## 2.9 Nanofiber mats characterization

The morphologies of the nanofiber mats were examined using a scanning electron microscope (SEM; JEOL, JSM-IT500HR, Tokyo, Japan) at an accelerating voltage of 15 kV. Prior to observation, the mats were coated with a thin layer of 24k gold to improve conductivity. The diameters of the nanofibers were analyzed using ImageJ software (version 1.54g).

## 3. Results and discussion

### 3.1 Response Surface Methodology (RSM) analysis

Subcritical ethanol extraction was performed by mixing Rang Jued powder with 50 ml of ethanol. A total of 15 experiments were designed using the Box–Behnken design (BBD). A summary of the experimental results is presented in Table 2.

**Table 2** The subcritical extraction using Box–Behnken design.

Variables	Amount of RJ powder		Temperature		Time		DPPH	TPC	DPPH	TPC
	unit	g/50 ml EtOH	°C	code	X <sub>2</sub>	code	X <sub>3</sub>	%	mg GAE/g	%
Run	X <sub>1</sub>	code	X <sub>2</sub>	code	X <sub>3</sub>	code	Predicted		Experimental	
1	1.5	-1	160	-1	15	0	79.13	21.34	78.32	21.35
2	1.9	+1	160	-1	15	0	86.03	19.73	88.79	20.91
3	1.5	-1	240	+1	15	0	48.76	16.21	46.01	15.03
4	1.9	+1	240	+1	15	0	50.52	12.90	51.50	12.89
5	1.5	-1	200	0	5	-1	89.74	28.10	91.54	28.86
6	1.9	+1	200	0	5	-1	94.58	26.14	92.64	25.73
7	1.5	-1	200	0	25	+1	90.51	29.10	92.45	29.52
8	1.9	+1	200	0	25	+1	94.18	26.14	92.38	25.38
9	1.7	0	160	-1	5	-1	79.29	19.22	78.32	18.45
10	1.7	0	240	+1	5	-1	54.42	15.78	55.38	16.20
11	1.7	0	160	-1	25	+1	87.63	22.26	86.67	21.83
12	1.7	0	240	+1	25	+1	46.29	13.74	47.11	14.52
13	1.7	0	200	0	15	0	93.25	30.55	93.15	30.48
14	1.7	0	200	0	15	0	93.25	30.55	93.26	30.49
15	1.7	0	200	0	15	0	93.25	30.55	93.33	30.69

DPPH scavenging activity and TPC from the trials were analyzed and used to generate second-order polynomial equations, as shown in equations 4 and 5. The predicted responses for DPPH scavenging activity and TPC were modeled as follows:

$$Y_{DPPH} = 93.25 + 2.12X_1 - 16.51X_2 + 0.09X_3 - 0.85X_1^2 - 26.24X_2^2 - 0.14X_3^2 - 1.25X_1X_2 - 0.29X_1X_3 - 4.16X_2X_3 \quad (4)$$

$$Y_{TPC} = 30.55 - 1.23X_1 - 2.99X_2 + 0.25X_3 - 1.69X_1^2 - 11.31X_2^2 - 1.49X_3^2 - 0.43X_1X_2 - 0.25X_1X_3 - 1.27X_2X_3 \quad (5)$$

where X<sub>1</sub>, X<sub>2</sub>, and X<sub>3</sub> represent the amount of Rang Jued powder, extraction temperature, and extraction time, respectively.

**Table 3** Analysis of variance (ANOVA) for quadratic model of DPPH.

Source	Sum of Squares	df	Mean Square	F-value	p-value	
<b>Model</b>	4851.98	9	539.11	78.61	< 0.0001	significant
A-RJ	36.11	1	36.11	5.27	0.0702	
B-Temp	2180.90	1	2180.90	317.99	< 0.0001	
C-Time	0.0671	1	0.0671	0.0098	0.9251	
AB	6.20	1	6.20	0.9046	0.3852	
AC	0.3435	1	0.3435	0.0501	0.8318	
BC	69.14	1	69.14	10.08	0.0247	
A <sup>2</sup>	2.70	1	2.70	0.3933	0.5581	
B <sup>2</sup>	2542.16	1	2542.16	370.67	< 0.0001	
C <sup>2</sup>	0.0728	1	0.0728	0.0106	0.9219	
<b>Residual</b>	34.29	5	6.86			
Lack of Fit	34.27	3	11.42	1344.45	0.0007	significant
Pure Error	0.0170	2	0.0085			
<b>Corr Total</b>	4886.27	14				

An analysis of variance (ANOVA) for the quadratic model of DPPH is shown in Table 3. The coefficient of determination (R<sup>2</sup>) for the model presented in Equation 4 was 0.9930, or approximately 99.3%, indicating a strong correlation between the predicted and experimental values of DPPH scavenging activity [33]. The model was statistically significant, with a p-value less than 0.0001 and an

F-value of 78.61. These results confirmed the model's reliability. Among the variables, extraction temperature ( $X_2$ ) was found to have a significant effect on DPPH scavenging activity, while the amount of Rang Jued powder ( $X_1$ ) and extraction time ( $X_3$ ) were not statistically significant.

Three-dimensional response surface and contour plots of DPPH were generated using Design-Expert software (Stat-Ease, Inc.). Figure 1 to illustrate the interaction between pairs of independent variables. The highest DPPH scavenging activity (93.33%) was observed when the extraction temperature was increased to 180–200°C. Beyond this range, DPPH activity slightly decreased, as shown in Figures 1 and 2. Figure 3 demonstrated that at the midpoint of the temperature range, DPPH scavenging activity increased with higher amounts of Rang Jued powder and longer extraction times.

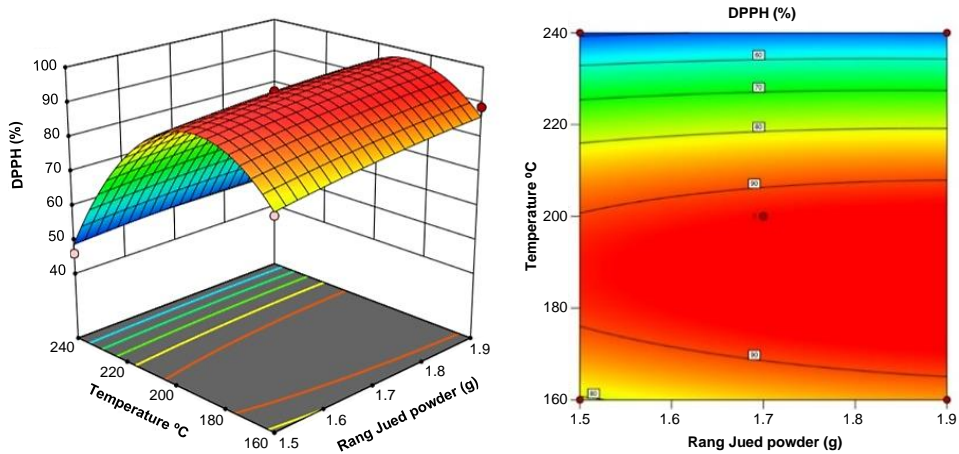


**Figure 1** Three-dimensional response surface and contour plots showing the relationship between Rang Jued powder and extraction temperature on DPPH scavenging activity.

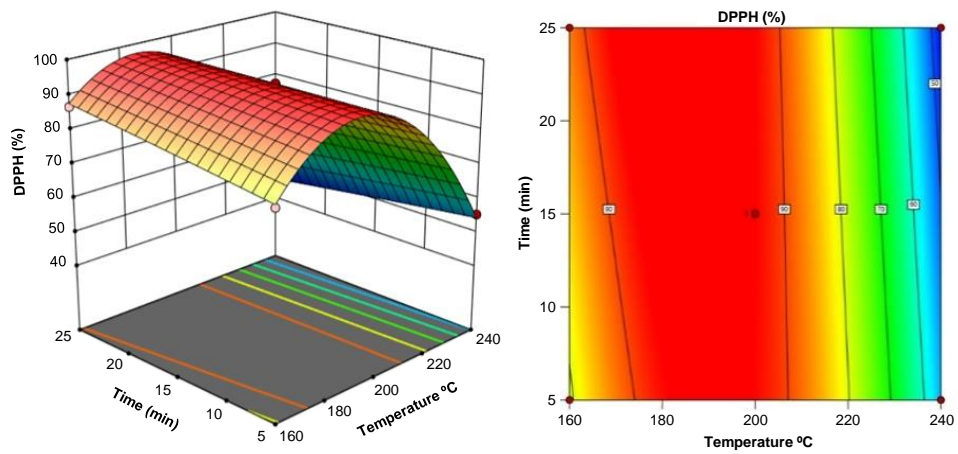


**Figure 2** Three-dimensional response surface and contour plots showing the relationship between extraction temperature and extraction time on DPPH scavenging activity.

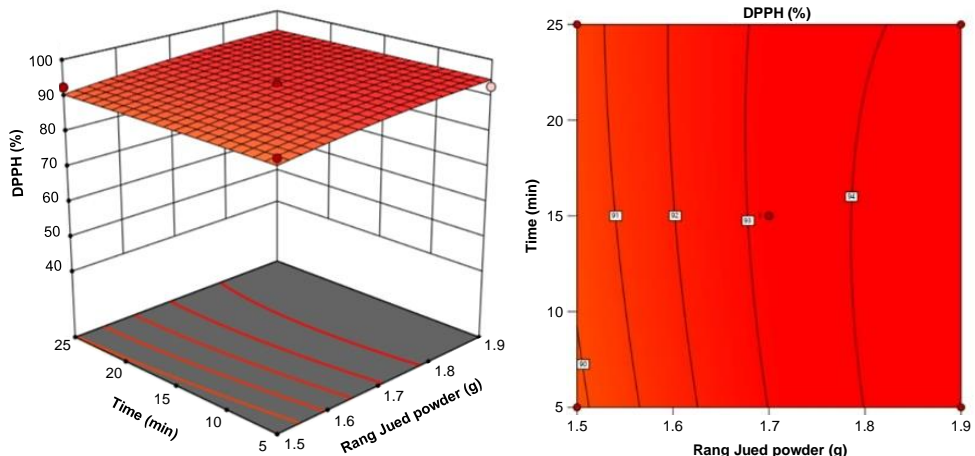


**Figure 3** Three-dimensional response surface and contour plots showing the relationship between Rang Jued powder and extraction time on DPPH scavenging activity.

Regarding the ANOVA results of TPC, the coefficient of determination ( $R^2$ ) for the model presented in Equation 5 was 0.9898, or approximately 98.98%, as shown in Table 4. The p-value was less than 0.05, indicating that the model was statistically significant. Specifically, the p-value of TPC was 0.0002, and the F-value was 53.68, confirming the significance of the results.

In addition, the amount of Rang Jued powder ( $X_1$ ) and extraction temperature ( $X_2$ ) were found to be significant parameters, while extraction time ( $X_3$ ) was not statistically significant—similar to the findings in the DPPH model. However, the extraction time remained an important factor, as longer durations were shown to degrade polyphenol contents [34].

**Table 4** Analysis of variance (ANOVA) for quadratic model of TPC.

Source	Sum of Squares	df	Mean Square	F-value	p-value	
<b>Model</b>	567.87	9	63.10	53.68	0.0002	significant
A-RJ	12.12	1	12.12	10.31	0.0237	
B-Temp	71.50	1	71.50	60.83	0.0006	
C-Time	0.4982	1	0.4982	0.4238	0.5438	
AB	0.7274	1	0.7274	0.6188	0.4671	
AC	0.2541	1	0.2541	0.2161	0.6615	
BC	6.42	1	6.42	5.46	0.0666	
$A^2$	10.60	1	10.30	9.02	0.03	
$B^2$	472.66	1	472.66	402.09	< 0.0001	
$C^2$	8.17	1	8.17	6.95	0.0462	
<b>Residual</b>	5.88	5	1.18			
Lack of Fit	5.85	3	1.95	133.24	0.0075	significant
Pure Error	0.0293	2	0.0146			
<b>Corr Total</b>	573.75	14				

From the 3D response surface and contour plots of TPC, (Figures 4 to 6), the highest TPC value of 30.69 mg GAE/g was observed. As shown in Figures 4 and 6, when the temperature increased beyond the 180–200 °C maximum point range, the TPC value decreased. Figure 5 showed that an extraction time of 15 minutes resulted in a higher TPC.

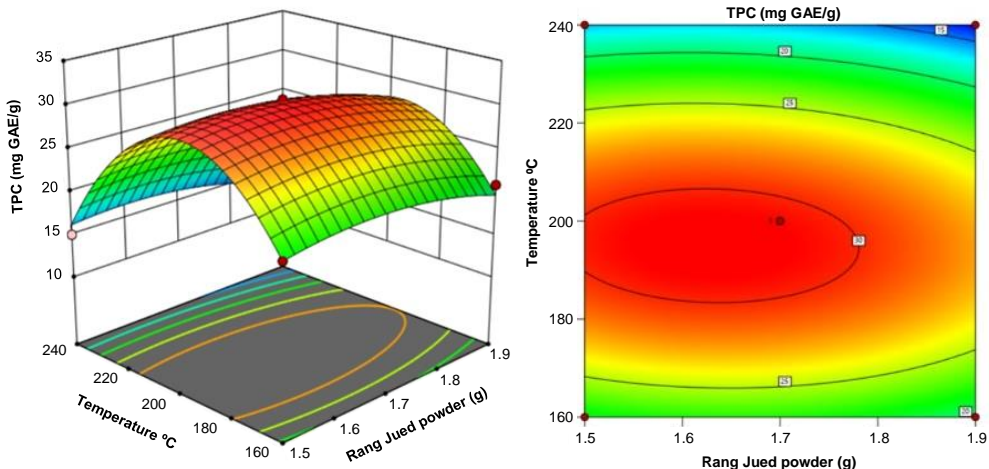


**Figure 4** Three-dimensional response surface and contour plots showing the relationship between Rang Jued powder and extraction temperature on TPC.

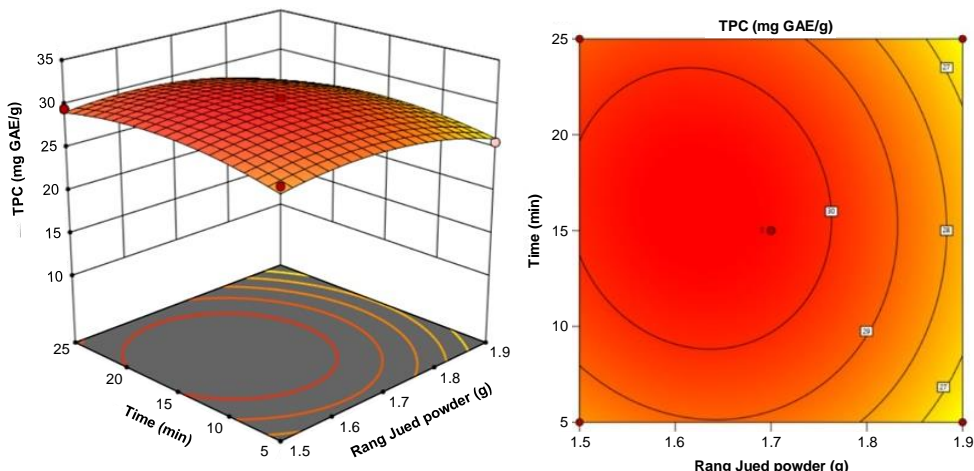


**Figure 5** Three-dimensional response surface and contour plots showing the relationship between Rang Jued powder and extraction time on TPC.

In addition, the findings of a previous study [12] on the extraction of defatted rice bran using subcritical aqueous ethanol supported these results. That study reported that DPPH scavenging activity and TPC increased up to 207 °C. Furthermore, the temperature had a strong effect on TPC, with peak values occurring between 180 to 220°C during subcritical ethanol extraction [35]. As the extraction temperature increased, the chemical properties of ethanol changed—viscosity, dielectric constant, and surface tension decreased, while diffusivity increased [36]. These changes enhanced diffusion, as the reduced viscosity and surface tension of subcritical ethanol improved mass transfer.

At high temperatures, TPC in olive extract increased due to reduced solvent viscosity. However, at excessively high temperatures, most phenolic compounds degraded due to their thermosensitive nature. Additionally, shorter extraction times yielded higher TPC values and maximum extract recovery [34].

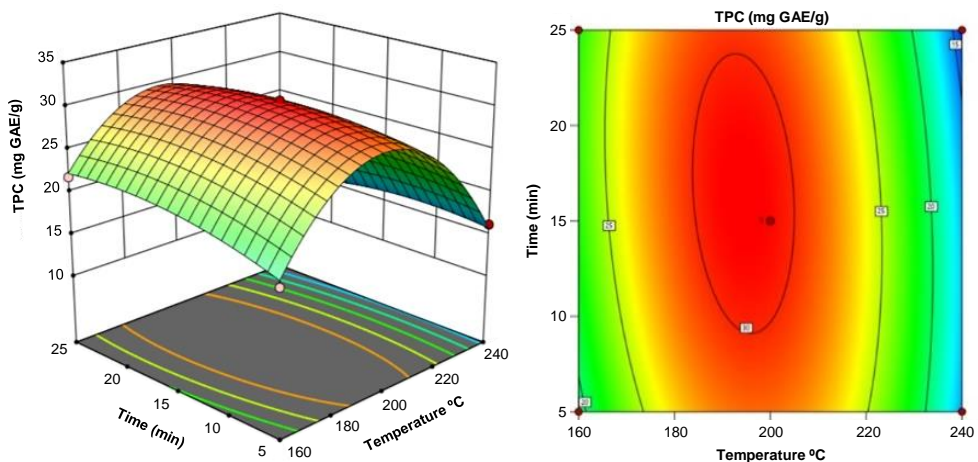


**Figure 6** Three-dimensional response surface and contour plots showing the relationship between extraction temperature and extraction time on TPC.

### 3.2 Optimization of subcritical extraction

The optimum conditions for subcritical ethanol extraction that yielded the highest DPPH scavenging activity and TPC were determined. According to the suggested model, the optimized value for each variable was 1.64 g of Rang Jued powder, an extraction temperature of 190 °C, and an extraction time of 15.14 min. These conditions predicted DPPH scavenging activity and TPC values of 95.02% and 30.77 mg GAE/g, respectively, compared with the experimental DPPH value of 94.91% and the experimental value of TPC of 30.35 mg GAE/g. Therefore, these conditions achieved near-maximum values for both DPPH and TPC, making them suitable for applications in tissue engineering, drug delivery, food packaging, and other application [37].

### 3.3 Swelling of nanofiber mats

The swelling behavior of nanofiber mats used as wound dressing was investigated through a swelling test, as determined by the exudate adsorption ability and capacity to maintain a moist wound environment [38, 39]. The crosslinked nanofiber mats were immersed in phosphate-buffered saline (PBS) at pH 7.4 for 24 h. After immersion, the PBS was removed, and the mats were weighed to assess their absorption capacity.

The swelling (%) results showed that swelling slightly increased as the voltage increased, and as the extract decreased, as shown in Table 3. At 45 kV—the voltage that resulted in the highest swelling—ratios of 7:3, 8:2, and 9:1, exhibited swelling values of 325.87%, 439.33%, and 441.07%, respectively. This trend was supported by the observation that the swelling degree of PVA/Chitosan-EDTA with *Garcinia mangostana* extract decreased with increasing amounts of the extract. This decrease was likely because the extract is a hydrophobic compound, which may reduce swelling properties [40].

Moreover, other researchers [14] reported that the swelling of PVA, PVA/*L. sativum* TEE extract, and PVA/polysaccharide slightly decreased due to intramolecular hydrogen bond interactions. Additionally, a low swelling ratio can negatively affect wound healing, as it may result in insufficient nutrient supply to heal the wound site. Therefore, achieving an appropriate swelling ratio supports the potential use of nanofiber mats containing antioxidant extract in wound healing applications [14, 41].

### 3.4 Antioxidant activity of the nanofibers

Antioxidants can neutralize reactive oxygen species (ROS); therefore, the wound healing process was promoted through the presence of antioxidant activity [42]. Antioxidants were extracted from plants such as *L. sativum* seeds, *Aloe vera*, and *Moringa oleifera*, which were rich in bioactive compounds such as phenolic compounds and flavonoids that supported wound healing process [14, 43]. Moreover, *Spirulina*-PCL nanofibers were fabricated as wound dressing. *Spirulina* exhibited antioxidant activity, which was used to prevent ROS-induced stress through antioxidant mechanisms. Additionally, *Spirulina* extract accelerated wounds regeneration [18].

The antioxidant extract was loaded into the nanofibers. Under optimum condition using subcritical extraction, the highest DPPH scavenging activity and TPC were achieved at 94.91% and 30.35 mg GAE/g, respectively. After fabrication, both non-crosslinked and crosslinked mats were evaluated. The results indicated that after crosslinking, DPPH scavenging activity increased, reaching a maximum value of 72.25%. However, TPC decreased to 0.59 mg GAE/g.

Furthermore, increasing the concentration of RJ extract enhanced antioxidant activity, with DPPH scavenging ranging from 67.64% to 72.25% and TPC ranging from 0.06 to 0.59 mg GAE/g. A high concentration of PVA resulted in lower antioxidant activity due to

the large surface area of the nanofibers [20]. A suitable nanofiber mat was identified based on its swelling and antioxidant activities. Higher extract concentrations led to increased antioxidant activity and enhanced swelling capacity [44].

### 3.5 Morphology of the nanofibers

The nanofibers were fabricated using the electrospinning technique. The morphologies of PVA/RJ extract composite nanofibers were investigated using scanning electron microscopy (SEM), as shown in Figure 7. The average diameter of nanofibers increased with the increment of PVA, meaning that a smaller average diameter was associated with a higher amount of RJ extract. These results were consistent with electrospun PVA/SLE extract nanofibers, where a lower PVA concentration resulted in a smaller average diameter [21].

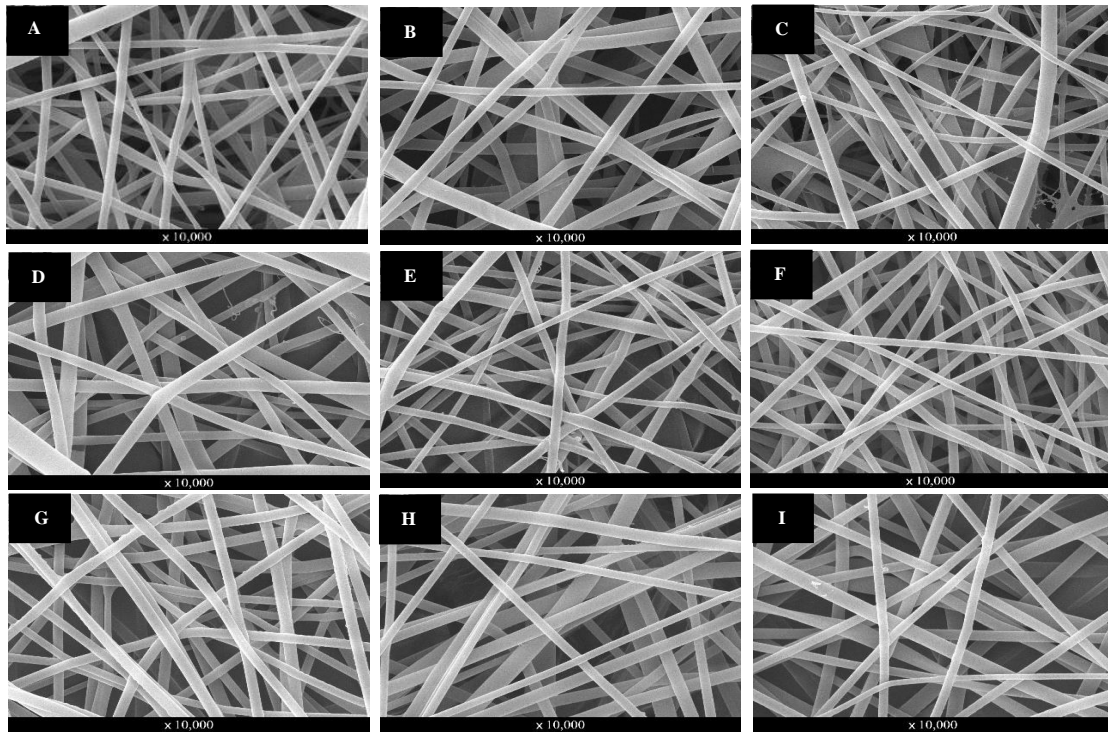


**Figure 7** Morphologies of PVA:RJ extract nanofibers at a 7:3 ratio under (a) 30 kV, (b) 35 kV, and (c) 45 kV; at 8:2 ratio under (d) 30 kV, (e) 35 kV, and (f) 45 kV; and at a 9:1 ratio under (g) 30 kV, (h) 35 kV, and (i) 45 kV.

The average diameters of each PVA/RJ ratio increased with voltage, ranging from 325 to 261 nm, 348 to 248 nm, and 377 to 359 nm, as shown in Table 5. The increase in voltage reduced the fiber diameter due to the influence of the electrical field [45]. Moreover, the fiber morphologies were smooth and beadless. Loading the extract did not affect the nanofiber morphology, including surface texture, uniformity, and bead formation [20, 40].

In addition, nanofibers loaded with RJ extract (7:3 ratio) demonstrated non-uniform fibers at 45 kV, as shown in Figure 7C. Under the same ratio, the nanofibers exhibited smoother fibers at lower voltage, as shown in Figure 7A and B. Furthermore, nanofibers loaded with RJ extract (8:2 ratio) at 45 kV showed the smallest diameter size of 248 nm and a high swelling ratio.

Furthermore, crosslinking improved the mechanical properties of the nanofibers, as the aldehyde groups in glutaraldehyde (GA) formed acetal bridges with the hydroxyl groups of PVA nanofibers [26]. After treatment, the nanofiber mats developed a yellowish color, and their morphology changed—becoming flattened and swollen, as shown in Figure 8. For example, the PVA/RJ nanofibers at a 7:3 ratio under 40 kV was crosslinked, and SEM images showed that the average diameter increased from 324 nm to 537 nm due to the GA reaction.

**Table 5** Electrospinning conditions, diameter size, swelling, DPPH, and TPC of nanofibers.

Ratio PVA:RJ	Voltage (kV)	Average diameter (nm)	Swelling (%)	DPPH (%)		TPC (mg GAE/g)	
				Non crosslink	Crosslink	Non crosslink	Crosslink
7:3	35	325.05	257.81	69.52	70.25	0.73	0.25
	40	324.34	299.56	70.33	72.25	1.00	0.59
	45	260.73	325.87	69.32	71.31	0.90	0.44
8:2	35	347.76	135.51	68.26	68.04	0.19	0.07
	40	346.90	380.19	68.57	69.82	0.67	0.57
	45	247.63	439.33	68.45	68.65	0.26	0.20
9:1	35	377.30	295.42	67.76	67.61	0.13	0.06
	40	361.65	382.30	68.24	69.09	0.32	0.26
	45	358.81	441.07	68.33	67.64	0.17	0.13

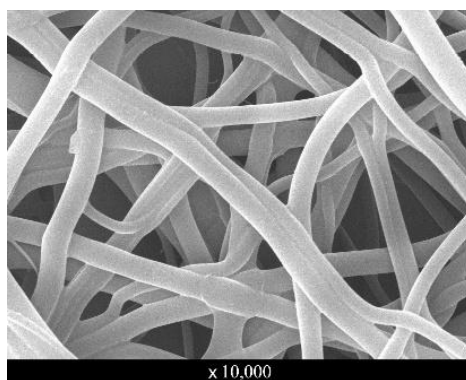


**Figure 8** Morphology of PVA:RJ extract nanofibers at a 7:3 ratio under 40 kV after crosslinking.

#### 4. Conclusion

Subcritical ethanol extraction was studied with Rang Jued leaf powder, and the variables affecting DPPH scavenging activity and TPC were investigated. These variables included the amount of Rang Jued powder (ranging from 1.5 to 1.9 g), extraction temperature (160 to 240 °C), and extraction time (5 to 25 min). The highest DPPH scavenging activity and TPC obtained were 94.91% and 30.35 mg GAE/g, respectively, at the optimum conditions of 1.64 g of Rang Jued powder, an extraction temperature of 190 °C, and an extraction time of 15.14 min.

Subcritical ethanol extraction proved to be an alternative technique for extracting and preserving antioxidants from Rang Jued leaves. The extract obtained under optimum conditions were successfully used to fabricate a wound dressing with PVA via the electrospinning process. The highest antioxidant activity of 72.25% was achieved at a 7:3 ratio of PVA:RJ extract under 40 kV. Under these conditions, the nanofiber had an average diameter of 324 nm and a swelling ratio of 300%. The high swelling capacity indicated that the nanofibers could retain more moisture, helping to keep the wound surface wet and thereby promoting the healing process.

#### 5. Acknowledgements

The authors wish to acknowledge research funding provided by the Thammasat School of Engineering, Faculty of Engineering, Thammasat University. We would also like to thank the Department of Chemical Engineering, Thammasat School of Engineering, Faculty of Engineering, Thammasat University.

#### 6. References

- [1] Tipduangta P, Julsrigival J, Chaithatwatthana K, Pongterdsak N, Tipduangta P, Chansakaow S. Antioxidant properties of Thai traditional herbal teas. *Beverages*. 2019;5(3):44.
- [2] Wanyo P, Chomnawang C, Huaisan K, Chamsai T. Comprehensive analysis of antioxidant and phenolic profiles of Thai medicinal plants for functional food and pharmaceutical development. *Plant Foods Hum Nutr*. 2024;79(2):394-400.
- [3] Essiedu JA, Gonu H, Adadi P, Withayagiat U. Polyphenols and antioxidant activity of *Thunbergia laurifolia* infused tea under drying conditions. *J Food Qual*. 2023;2023(1):5046880.
- [4] Junsi M, Siripongvutikorn S. *Thunbergia laurifolia*, a traditional herbal tea of Thailand: botanical, chemical composition, biological properties and processing influence. *Int Food Res J*. 2016;23(3):923-7.
- [5] Woottisin N, Kongkiatpaiboon S, Sukprasert S, Sathirakul K. Development and validation of stability indicating HPLC method for determination of caffeic acid, vitexin and rosmarinic acid in *Thunbergia laurifolia* leaf extract. *Pharmacogn J*. 2020;12(3):611-8.
- [6] Suwanchaikasem P, Chaichantipyuth C, Sukrong S. Antioxidant-guided isolation of rosmarinic acid, a major constituent from *Thunbergia laurifolia*, and its use as a bioactive marker for standardization. *Chiang Mai J Sci*. 2014;41(1):117-27.
- [7] Onsawang T, Suwanvecho C, Sithisarn P, Phechkrajang C, Rojsanga P. Experimental design approach for the quantitative analysis of multicomponents by single marker and HPLC fingerprinting of *Thunbergia laurifolia* aqueous extract. *Phytochem Anal*. 2024;35(6):1472-85.
- [8] Chaiyana W, Chansakaow S, Intasai N, Kiattisin K, Lee KH, Lin WC, et al. Chemical constituents, antioxidant, anti-MMPs, and anti-hyaluronidase activities of *Thunbergia laurifolia* Lindl. leaf extracts for skin aging and skin damage prevention. *Molecules*. 2020;25(8):1923.
- [9] Fadimu GJ, Ghafoor K, Babiker EE, Al-Juhaimi F, Abdulraheem RA, Adenekan MK. Ultrasound-assisted process for optimal recovery of phenolic compounds from watermelon (*Citrullus lanatus*) seed and peel. *J Food Meas Charact*. 2020;14:1784-93.
- [10] Yoswathanan N, Eshtiaghi MN. Optimization of subcritical ethanol extraction for xanthone from mangosteen pericarp. *Int J Chem Eng Appl*. 2015;6(2):115-9.
- [11] Plangklang T, Khuwijitjaru P, Klinchongkon K, Adachi S. Chemical composition and antioxidant activity of oil obtained from coconut meal by subcritical ethanol extraction. *J Food Meas Charact*. 2021;15(5):4128-37.
- [12] Chiou TY, Neoh TL, Kobayashi T, Adachi S. Properties of extract obtained from defatted rice bran by extraction with aqueous ethanol under subcritical conditions. *Food Sci Technol Res*. 2012;18(1):37-45.
- [13] Sriyanti I, Jauhari J. Electrospun of poly(vinyl alcohol) nanofiber as carrier of *Garcinia mangostana* L. pericarp extract. *J Phys: Conf Ser*. 2019;1170:012056.
- [14] Amer AA, Mohammed RS, Hussein Y, Ali ASM, Khalil AA. Development of *Lepidium sativum* extracts/PVA electrospun nanofibers as wound healing dressing. *ACS Omega*. 2022;7(24):20683-95.

- [15] Mouro C, Gomes AP, Gouveia IC. Emulsion electrospinning of PLLA/PVA/Chitosan with *Hypericum perforatum* L. as an antibacterial nanofibrous wound dressing. *Gels.* 2023;9(5):353.
- [16] Quintero-Borregales LM, Vergara-Rubio A, Santos A, Famá L, Goyanes S. Black tea extracts/polyvinyl alcohol active nanofibers electrospun mats with sustained release of polyphenols for food packaging applications. *Polymers.* 2023;15(5):1311.
- [17] Marjani ME, Shirazi RHMT, Mohammadi T. CDI crosslinked chitosan/poly (vinyl alcohol) electrospun nanofibers loaded with *Achillea millefolium* and Viola extract: a promising wound dressing. *Carbohydr Polym.* 2024;336:122117.
- [18] Jung SM, Min SK, Lee HC, Kwon YS, Jung MH, Shin HS. Spirulina-PCL nanofiber wound dressing to improve cutaneous wound healing by enhancing antioxidative mechanism. *J Nanomater.* 2016;2016(1):6135727.
- [19] Maleki H, Doostan M, Khoshnevisan K, Baharifar H, Maleki SA, Fatahi MA. *Zingiber officinale* and *thymus vulgaris* extracts co-loaded polyvinyl alcohol and chitosan electrospun nanofibers for tackling infection and wound healing promotion. *Heliyon.* 2024;10(1):e23719.
- [20] Doostan M, Doostan M, Mohammadi P, Khoshnevisan K, Maleki H. Wound healing promotion by flaxseed extract-loaded polyvinyl alcohol/chitosan nanofibrous scaffolds. *Int J Biol Macromol.* 2023;228:506-16.
- [21] Aruan NM, Sriyanti I, Edikresnha D, Suciati T, Munir MM, Khairurrijal. Polyvinyl alcohol/soursop leaves extract composite nanofibers synthesized using electrospinning technique and their potential as antibacterial wound dressing. *Procedia Eng.* 2017;170:31-5.
- [22] Sim P, Strudwick XL, Song YM, Cowin AJ, Garg S. Influence of acidic pH on wound healing in vivo: a novel perspective for wound treatment. *Int J Mol Sci.* 2022;23(21):13655.
- [23] Bagheri M, Validi M, Gholipour A, Makvandi P, Sharifi E. Chitosan nanofiber biocomposites for potential wound healing applications: antioxidant activity with synergic antibacterial effect. *Bioeng Transl Med.* 2022;7(1):e10254.
- [24] Wonkchalee O, Boonmars T, Aromdee C, Laummaunwai P, Khunkitti W, Vaeteewoottacharn K, et al. Anti-inflammatory, antioxidant and hepatoprotective effects of *Thunbergia laurifolia* Linn. on experimental opisthorchiasis. *Parasitol Res.* 2012;111(1):353-9.
- [25] Chitkrachang N, Panthong S, Ploysombun S, Choosrichom S, Ngamkham N, Kwanchian D, et al. A comparison of antibacterial activity against acne-inducing bacteria, anti-inflammatory activity, and total phenolic content of fresh and dried leaves of *Thunbergia laurifolia* Lindl extracts. *J Thai Trad Alt Med.* 2023;21(2):356-66. (In Thai)
- [26] Destaye AG, Lin CK, Lee CK. Glutaraldehyde vapor cross-linked nanofibrous PVA mat with in situ formed silver nanoparticles. *ACS Appl Mater Interfaces.* 2013;5(11):4745-52.
- [27] Teixeira MA, Antunes JC, Amorim MTP, Felgueiras HP. Green optimization of glutaraldehyde vapor-based crosslinking on poly (vinyl alcohol)/cellulose acetate electrospun mats for applications as chronic wound dressings. *Proceedings.* 2021;69(1):30.
- [28] Truong YB, Choi J, Mardel J, Gao Y, Maisch S, Musameh M, et al. Functional cross-linked electrospun polyvinyl alcohol membranes and their potential applications. *Macromol Mater Eng.* 2017;302(8):1700024.
- [29] Charernsriwilaiwat N, Rojanarata T, Ngawhirunpat T, Opanasopit P. Electrospun chitosan/polyvinyl alcohol nanofibre mats for wound healing. *Int Wound J.* 2014;11(2):215-22.
- [30] Huang SM, Liu SM, Tseng HY, Chen WC. Effect of citric acid on swelling resistance and physicochemical properties of post-crosslinked electrospun polyvinyl alcohol fibrous membrane. *Polymers.* 2023;15(7):1738.
- [31] Balyan S, Mukherjee R, Priyadarshini A, Vibhuti A, Gupta A, Pandey RP, et al. Determination of antioxidants by DPPH radical scavenging activity and quantitative phytochemical analysis of *Ficus religiosa*. *Molecules.* 2022;27(4):1326.
- [32] Ibrahim UK, Yusof MIS, Zamil KAA, Kamarrudin N, Maqsood-ul-Haque SNS, Ab Rashid SR. Total phenolic content and antioxidant activity of local fruit wastes in Malaysia. *Adv Mater Res.* 2015;1113:471-6.
- [33] Prgomet I, Gonçalves B, Domínguez-Perles R, Pascual-Seva N, Barros AIRNA. A Box-Behnken design for optimal extraction of phenolics from almond by-products. *Food Anal Methods.* 2019;12:2009-24.
- [34] Martin-Garcia B, Pimentel-Moral S, Gómez-Caravaca AM, Arráez-Román D, Segura-Carretero A. Box-Behnken experimental design for a green extraction method of phenolic compounds from olive leaves. *Ind Crops Prod.* 2020;154:112741.
- [35] Bodoira R, Velez A, Andreatta AE, Martínez M, Maestri D. Extraction of bioactive compounds from sesame (*Sesamum indicum* L.) defatted seeds using water and ethanol under sub-critical conditions. *Food Chem.* 2017;237:114-20.
- [36] Sulejmanović M, Jerković I, Zloh M, Nastić N, Milić N, Drljača J, et al. Supercritical fluid extraction of ginger herbal dust bioactives with an estimation of pharmacological potential using *in silico* and *in vitro* analysis. *Food Biosci.* 2024;59:104074.
- [37] Faki R, Gursoy O, Yilmaz Y. Effect of electrospinning process on total antioxidant activity of electrospun nanofibers containing grape seed extract. *Open Chem.* 2019;17:912-8.
- [38] Anaya-Mancipe JM, Queiroz VM, Dos Santos RF, Castro RN, Cardoso VS, Vermelho AB, et al. Electrospun nanofibers loaded with *Plantago major* L. extract for potential use in cutaneous wound healing. *Pharmaceutics.* 2023;15(4):1047.
- [39] Sarhan WA, Azzazy HM, El-Sherbiny IM. Honey/chitosan nanofiber wound dressing enriched with *Allium sativum* and *Cleome drosierifolia*: enhanced antimicrobial and wound healing activity. *ACS Appl Mater Interfaces.* 2016;8(10):6379-90.
- [40] Charernsriwilaiwat N, Rojanarata T, Ngawhirunpat T, Sukma M, Opanasopit P. Electrospun chitosan-based nanofiber mats loaded with *Garcinia mangostana* extracts. *Int J Pharm.* 2013;452(1-2):333-43.
- [41] Ko SW, Lee JY, Lee J, Son BC, Jang SR, Aguilar LE, et al. Analysis of drug release behavior utilizing the swelling characteristics of cellulosic nanofibers. *Polymers.* 2019;11(9):1376.
- [42] Vilchez A, Acevedo F, Cea M, Seeger M, Navia R. Applications of electrospun nanofibers with antioxidant properties: a review. *Nanomaterials.* 2020;10(1):175.
- [43] Fayemi OE, Ekennia AC, Katata-Seru L, Ebokaiwe AP, Ijomone OM, Onwudiwe DC, et al. Antimicrobial and wound healing properties of polyacrylonitrile-moringa extract nanofibers. *ACS Omega.* 2018;3(5):4791-7.
- [44] Sadri M, Arab-Sorkhi S, Vatani H, Bagheri-Pebdeni A. New wound dressing polymeric nanofiber containing green tea extract prepared by electrospinning method. *Fibers Polym.* 2015;16:1742-50.
- [45] Golkar P, Kalani S, Allafchian AR, Mohammadi H, Jalali SAH. Fabrication and characterization of electrospun *Plantago major* seed mucilage/PVA nanofibers. *J Appl Polym Sci.* 2019;136(32):47852.